J|A|C|S ARTICLES

Published on Web 12/04/2008

A Predicted Organometallic Series Following a 32-Electron Principle: An@C_{28} (An = Th, Pa^+, U^{2+}, Pu^{4+})

Jean-Pierre Dognon,*,† Carine Clavaguéra,‡ and Pekka Pyykkö*,‡,§

CEA/Saclay, DSM/DRECAM/SCM, 91191 Gif-sur-Yvette, France, Laboratoire des Mécanismes Réactionnels, Ecole Polytechnique, CNRS, 91128 Palaiseau Cedex, France, and Department of Chemistry, University of Helsinki, P.O. Box 55, 00014 Helsinki, Finland

Received August 28, 2008; E-mail: jean-pierre.dognon@cea.fr; pekka.pyykko@helsinki.fi

Abstract: The spectroscopic and thermodynamic properties of the molecules M@C_{28} (M = Ce, Th, Pa^+, U^{2+}, Pu^{4+}) are calculated using density functional theory. The systems have considerable energetic stability. It is shown that the actinide cases can be classified as "32-electron" systems, using the bonding s-, p-, d-, and f-type orbitals of the central metal. The rest of the valence molecular orbitals have purely carbon character.

Introduction

The 18-electron principle is well-known in inorganic and organometallic chemistry. A recent discussion of its origin and interpretation is provided in ref 1. Is it possible to go to the next step, systems obeying a 32-electron principle? Obviously, an f element would then have to be used as the central atom.

We recently proposed a series of intermetallic cluster compounds An@Pb_{12} (An = Pu, Am^+), which fulfilled all of the necessary criteria to be justly called a 32-electron system.[2] In particular, separated by a large gap from the lower-lying Pb 6s band, there was a 32-electron valence band with Pb 6p orbitals bonding to the An 7s, 7p, 6d, and 5f orbitals, exactly as required. The calculated HOMO−LUMO gap was also large.

We now report a theoretical study of another series, the organometallic complexes An@C_{28} (An = Th, Pa^+, U^{2+}, Pu^{4+}), whose electron count also has a chance of exactly fulfilling a 32-electron principle. As pointed out by Rösch in a study of Ce@C_{28},[3] the metal atom then contributes four electrons and each of the 28 carbons one π electron (where π is defined with respect to the approximate sphere surface). Because Ce is an early lanthanide, for which the 4f shell, being nodeless, is very compact, it is especially unlikely that all 14 occupied molecular orbitals (MOs) with f-type symmetry could have significant Ce 4f participation. It should be noted that each of them can in principle have both metal and ligand character. The related system U@C_{28} actually forms spontaneously in the gas phase.[4] Its properties have been theoretically analyzed by Pitzer and co-workers,[5,6] who were mainly interested in the electronic states arising from the two extra electrons, which are distributed between the nearly pure actinide 5f orbitals and the carbon 2p shell. An earlier local density approximation treatment[7] of M@C_{28} (M = Sn, Zr, U) has already mentioned the possibility of 5f participation in bonding in the actinides (M = Th, Pu). In view of the fact that C_{28} was "slightly too small" for the earlier actinides, it is interesting that chromatographic, UV/vis/IR and XANES experimental data already exist[8] for another tetrahedral cage, An@C_{82}. The question is, can one find sufficiently well-defined bonding orbitals, corresponding just to the 32-electron idea and excluding other bonding orbitals, in this family of known or potential compounds? Moreover, can one point out any specific molecular properties associated with these 32-electron compounds?

Theoretical Calculations

The cluster geometries were optimized with the Amsterdam Density Functional (ADF) program (version 2007.01)[9] using the Perdew−Burke−Ernzerhof (PBE)[10] generalized gradient approximation exchange-correlation functional. Both scalar and spin−orbit relativistic corrections were included via the ZORA model.[11] For the computation of the exchange-correlation potential, the true density was used instead of the default density-fitting procedure in order to obtain better accuracy and stability with actinide elements. Vibrational frequencies were calculated to confirm that the structures are true minima on the potential energy surfaces. DFT/B3LYP[12] single-point energy calculations were performed at the DFT/PBE-optimized geometry to take into account the Hartree−Fock exchange effects on the bonding energy. The TZ2P Slater basis

† CEA/Saclay.
‡ Ecole Polytechnique.
§ University of Helsinki.

(1) Pyykkö, P. *J. Organomet. Chem.* **2006**, *691*, 4336–4340.
(2) Dognon, J. P.; Clavaguéra, C.; Pyykkö, P. *Angew. Chem., Int. Ed.* **2007**, *46*, 1427–1430.
(3) Rösch, N.; Häberlen, O. D.; Dunlap, B. I. *Angew. Chem., Int. Ed. Engl.* **1993**, *32*, 108–110.
(4) Guo, T.; Diener, M. D.; Chai, Y.; Alford, M. J.; Haufler, R. E.; McClure, S. M.; Ohno, T.; Weaver, J. H.; Scuseria, G. E.; Smalley, R. E. *Science* **1992**, *257*, 1661–1664.
(5) Tuan, D. F. T.; Pitzer, R. M. *J. Phys. Chem.* **1995**, *99*, 15069–15073.
(6) Zhao, K.; Pitzer, R. M. *J. Phys. Chem.* **1996**, *100*, 4798–4802.
(7) Jackson, K.; Kaxiras, E.; Pederson, M. R. *J. Phys. Chem.* **1994**, *98*, 7805–7810.
(8) Akiyama, K.; Sueki, K.; Tsukada, K.; Yaita, T.; Miyake, Y.; Haba, H.; Asai, M.; Kodama, T.; Kikuchi, K.; Ohtsuki, T.; Nagame, Y.; Katada, M.; Nakahara, H. *J. Nucl. Radiochem. Sci.* **2002**, *3*, 151–154.
(9) *ADF*, version 2007.01; SCM: Amsterdam, 2007.
(10) Perdew, J. P.; Burke, K.; Ernzerhof, M. *Phys. Rev. Lett.* **1996**, *77*, 3865–3868.
(11) van Lenthe, E.; Baerends, E. J.; Snijders, J. G. *J. Chem. Phys.* **1993**, *99*, 4597–4610.
(12) Becke, A. D. *J. Chem. Phys.* **1993**, *98*, 5648–5652.

 10.1021/ja806811p CCC: $40.75

sets (relativistic valence triple-ζ with two polarization functions) were employed, and the frozen-core approximation was applied to all of the atoms, resulting in 4, 12, 12, 13, 14, and 16 electrons for the C, Ce, Th, Pa, U, and Pu atoms, respectively. The Morokuma-type decomposition of the bonding energy[13] into the Pauli (exchange) repulsion, total steric interaction, and orbital interaction terms was used to analyze the electronic structure and the bonding properties in the clusters. Calculations of the electron localization function (ELF) were performed with the DGrid 4.3 program.[14] The Voronoi deformation density (VDD) charges were calculated in order to evaluate the charge rearrangements due to the formation of the complex from the actinide and C_{28} fragments. The VDD calculates the flow of electron density to or from a certain atom or fragment due to bond formation.[15]

It should be noted that except for the empty C_{28} cage and the neutral complex $U@C_{28}$, the present species have closed electronic shells.

Results and Discussion

1. Chemical Stabilization of the Clusters. The chemical stabilization of the C_{28} cage is known experimentally,[16] as it is the smallest even-numbered fullerene that forms with abundance in condensing carbon vapors. It is the most symmetrical possible structure for 28 atoms: a triplet of pentagons arranged at each vertex of a tetrahedron in the symmetry point group T_d. The ground electronic state of the tetrahedron C_{28} was found to be $^5A_2$, with one electron in an a_1 orbital and three in a t_2 orbital,[6] corresponding to a bond located at each of the four carbons at the tetrahedral vertices of the T_d structure. In our TZ2P basis set calculations, the three symmetry-inequivalent equilibrium bond lengths were calculated to be 146.6, 140.0, and 153.9 pm. The next two excited electronic states of C_{28} in the SCF-RHF calculations, $^1A_1$ and $^3T_1$, were found to lie at considerably higher energies (3.2 and 4.1 eV, respectively).[6] The only other possible isomer of C_{28} was found to be a structure having D_2 symmetry that also lies considerably higher in energy.[6]

Endohedral clusters encapsulating a lanthanide or an actinide atom were also formed under specific experimental conditions, and the best known of these is $U@C_{28}$.[4] The efficiency of formation of $U@C_n$ metallofullerenes in the described experiments is remarkable. Photoemission spectra for the valence bands of sublimed films of fullerenes showed a strong uranium 5f emission. This was originally interpreted[4] as evidence for U(IV) with a $5f^2$ configuration. Zhao and Pitzer[6] actually found a distributed $(5f)^1(C\ shell)^1$ dominant contribution. As discussed now, one furthermore has a large 5f participation in the filled bonding orbitals. The 5f signature was consistent with a formal 4+ valence state, in agreement with the assertion that a tetravalent atom has stabilized the fullerene. A large diversity of new molecules and materials may therefore ultimately be available if these C_{28} fullerene and $M@C_{28}$ metallofullerenes are used as building blocks on a nanometer scale.

Our theoretical study of the $M@C_{28}$ (M = Ce, Th, Pa^+, U^{2+}, Pu^{4+}) metallofullerenes confirms the expected chemical stabilization. As for $M@Pb_{12}$ clusters,[2] the influence of the cation in the cage and the cluster stabilization can be gauged by the geometric deformation and the energy difference between the HOMO and LUMO orbitals. Figure 1 shows the geometric structures of the empty cage and the cage filled with the Pu^{4+} ion. The deformation of the cage due to addition of the Pu^{4+} ion is seen to be small. For the other elements, the behavior is similar, and the M−C distances given in Table 1 show a slight radial expansion of up to 11 pm in the initial cage radius. It is also important to notice that the T_d symmetry is preserved in each case, in spite of two or three different values of the M−C distance according to the nature of the cluster. The HOMO−LUMO gap (2−4 eV for all of the endohedral clusters) is large in comparison with the smaller gap (<1 eV) for the empty C_{28} cage, conferring a first indication of the chemical stability of these systems. These values are at least as large as those for $M@Pb_{12}$.[2] Concerning the occupations of the 4f/5f orbitals, we give in Table 1 both the number of electrons in the "pure" f MOs and the total f-type Mulliken population. The difference between the two comes from f character in the bonding MOs.

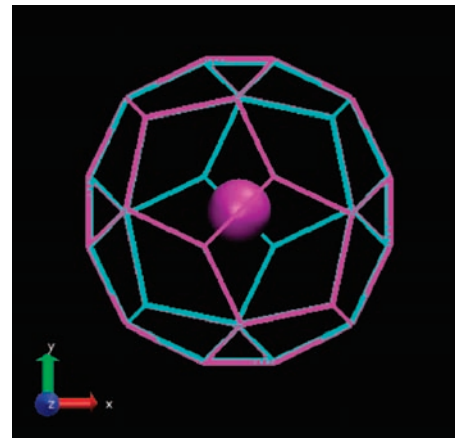

Figure 1. Geometric cage deformation due to placing a Pu atom inside the C_{28} cage. $Pu^{4+}@C_{28}$ is shown in purple and the empty C_{28} cage in cyan.

Table 1. Distances between the Central Atom and the Carbon Atoms of the Cage [for the Empty Cage, *r*(M−C) Is the Radius of the Cage], HOMO−LUMO Gaps, and 4f/5f Orbital Occupation Numbers

actinide	method	HOMO−LUMO gap (eV)	*r*(M−C) (pm)	4f/5f metal occupation	4f/5f orbital occupation
C_{28}	PBE	0.2	241.4/243.4	−	−
	B3LYP	0.8	−	−	−
$Ce@C_{28}$	PBE	2.4	246.1/253.1	1	1.9
	B3LYP	3.5	−	−	1.7
$Th@C_{28}$	PBE	2.4	248.1/254.5	0	2.1
	B3LYP	3.5	−	−	2.0
$Pa^+@C_{28}$	PBE	2.6	246.5/252.4	2	2.8
	B3LYP	3.7	−	−	2.8
$U^{2+}@C_{28}$	PBE	2.9	244.8/245.6/250.6	3	3.9
	B3LYP	4.0	−	−	3.8
$Pu^{4+}@C_{28}$	PBE	2.7	244.1/245.7/248.9	4	5.9
	B3LYP	3.9	−	−	5.9

Figure 2 shows a detailed graphical analysis of the electronic bonding energy of each $M@C_{28}$ cluster with respect to the atomic dissociation limit $M + C_{28}$ for M = Ce and Th and to the ionic dissociation limit $M^{n+} + C_{28}$ for $M^{n+} = Pa^+$, U^{2+}, and Pu^{4+}. Each of the clusters studied is a very stable system, with a bonding energy between 11 and 38 eV. The electrostatic and Pauli repulsion energy terms follow the behavior of the interaction between the two charges, and the global steric term (i.e., electrostatic plus Pauli repulsion) is minimal for the Pu^{4+} cluster. In all cases, the orbital interaction energy is large,

(13) Bickelhaupt, F. M.; Baerends, E. J. In *Reviews in Computational Chemistry*; Wiley-VCH: New York, 2000; Vol. 15, pp 1−86.
(14) Kohout, M. *DGrid*, version 4.3; Max-Planck Institut für Chemische Physik fester Stoffe: Dresden, Germany, 2008.
(15) Guerra, C. F.; Handgraaf, J. W.; Baerends, E. J.; Bickelhaupt, F. M. *J. Comput. Chem.* **2004**, *25*, 189–210.
(16) Kaxiras, E.; Zeger, L. M.; Antonelli, A.; Juan, Y. M. *Phys. Rev. B* **1994**, *49*, 8446–8453.

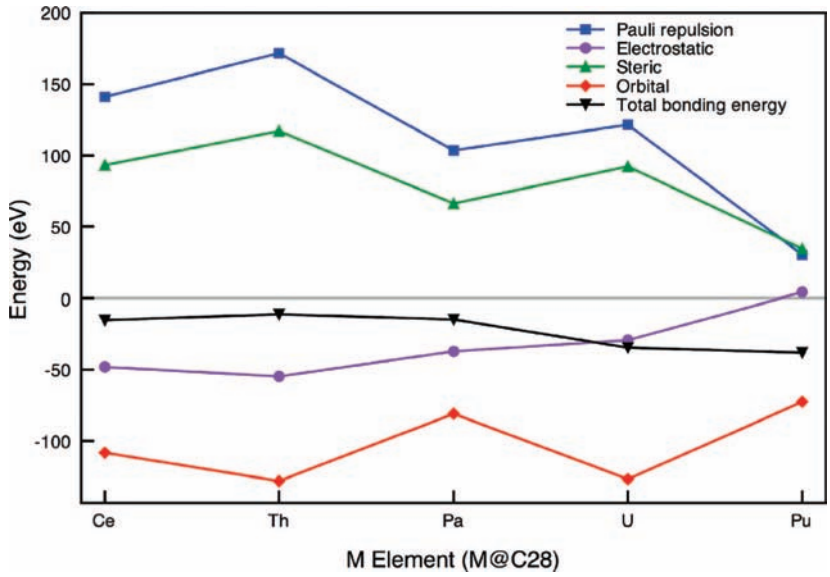

Figure 2. Bonding energy analysis for the $M@C_{28}$ clusters (M = Ce, Th, Pa^{+}, U^{2+}, Pu^{4+}).

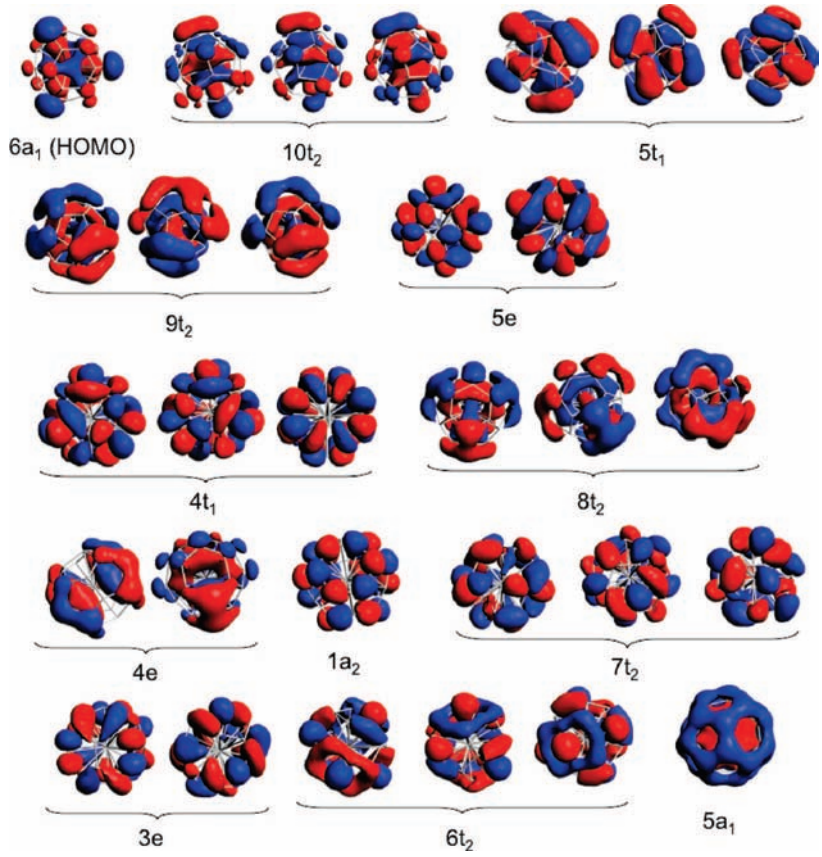

Figure 3. Valence MOs of $Pu^{4+}@C_{28}$.

showing a nonsimple electrostatic interaction and real chemical bonding that involves both cage and central-atom orbitals. In the U^{2+} and Pu^{4+} cases, the VDD analysis exhibits strong charge transfers of −1.42 and −1.37 electrons, respectively, from the cage to the actinide orbitals. In the other clusters, the VDD values range only from 0 to −0.3 electrons. The thermodynamic stabilities are discussed in section 5 below.

2. Electronic Structures of the Clusters. In Figure 3, the $Pu^{4+}@C_{28}$ valence MOs are plotted in descending energetic order. One can see the overlap between the Pu atomic orbitals and the C_{28} cage orbitals in the $6a_1$, $10t_2$, $5t_1$, $9t_2$, $8t_2$, 4e, and $5a_1$ valence molecular orbitals. This can be related to a strong participation of the central-atom orbitals in these 16 MOs, involving 32 electrons. The other molecular orbitals are pure C_{28} cage orbitals that do not interact with the metal center. Consequently, the 7s, 7p, 6d, and 5f orbitals of the Pu^{4+} ion all hybridize with the C_{28} cage orbitals. Symmetrized fragment orbitals (SFOs)[17] were used for the analysis of the MOs, giving a useful description of their character. The SFO contributions per MO are largest for the 5f atomic orbitals: 46, 41, and 31%

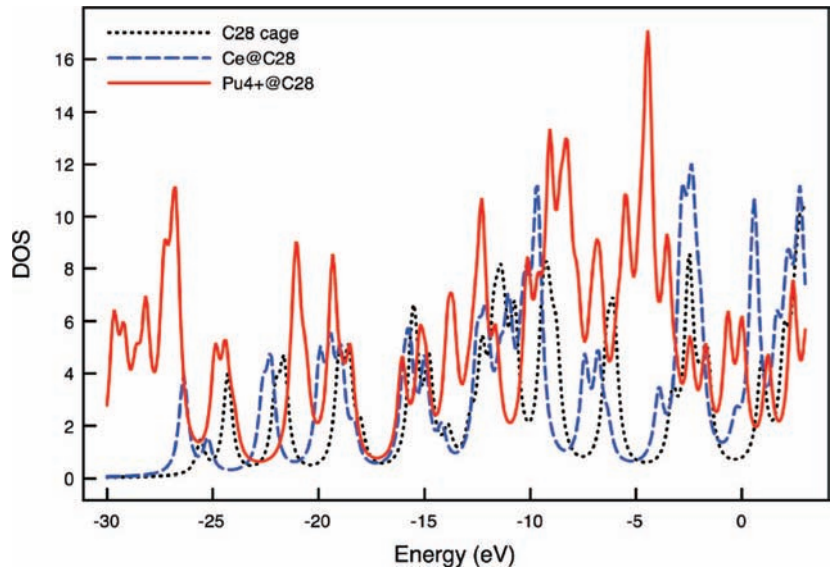

Figure 4. Densities of states for the C_{28} cage (for α orbitals), Ce@C_{28}, and Pu^{4+}@C_{28} as a function of the orbital energy.

for the $6a_1$, $10t_2$, and $5t_1$ MOs, respectively. The $9t_2$ and $8t_2$ MOs also mix 6d and 7p orbitals with the 2p(C) orbitals of the cage. The 4e and $5a_1$ MOs correspond to 6d and 7s orbitals, respectively, each one hybridizing with the cage. The energy spectrum is similar for An = Th, Pa, U. From Th to Pu, the 5f orbital participation in the bonding $6a_1$, $10t_2$, and $5t_1$ MOs increases from 9 to 46%. Following our discussion on An@Pb_{12} (An = Pu, Am) clusters,[2] the present endohedral fullerene clusters are the second illustration of the 32-electron principle. In the case of the lanthanide cluster Ce@C_{28}, the 4f levels lie close to highest occupied molecular orbitals but do not strongly hybridize with the fullerene cage. The SFO analysis gives only a slight hybridization of the 4f orbitals (∼6−8%) and a quasi-negligible hybridization of the 6p orbitals. This system is hence not a good example of the 32-electron rule.

The densities of states (DOS) of the C_{28} cage and the Ce@C_{28} and Pu^{4+}@C_{28} clusters are plotted in Figure 4. The curves for the C_{28} cage and the Ce@C_{28} are very similar, whereas the Pu^{4+}@C_{28} curve is shifted deeper in energy as a result of the actinide/cage-orbital bonding. Cut-plane representations of the ELFs for C_{28}, Ce@C_{28}, Th@C_{28}, Pa^{+}@C_{28}, U^{2+}@C_{28}, and Pu^{4+}@C_{28} are given in Figure 5. The various ELF representations differ strongly: in the C_{28} and Ce@C_{28} cases, the basins are located around the carbon atoms, with a large hole in the center of the empty cage and around the Ce atom in the endohedral cluster. For the actinide systems, and in particular for Pu^{4+}, a local electron maximum exists between the central atom and the C atoms of the cage, indicating strong bonding.

In summary, the present actinide-containing clusters all qualify as 32-electron species.

3. Spin−Orbit Effects. The bonding of plutonium has been shown in some cases to be influenced by spin−orbit coupling.[18] To evaluate these effects in the Pu^{4+}@C_{28} cluster, extensive spin−orbit coupling studies were performed, including a geometry optimization, SFO analysis, and bonding energy analysis at the DFT/PBE level. Spin−orbit coupling effects cause a maximum expansion of the Pu−C distance of ∼2.7 pm with respect to the scalar relativistic distances. A slight effect on the HOMO−LUMO gap exists, decreasing the value from

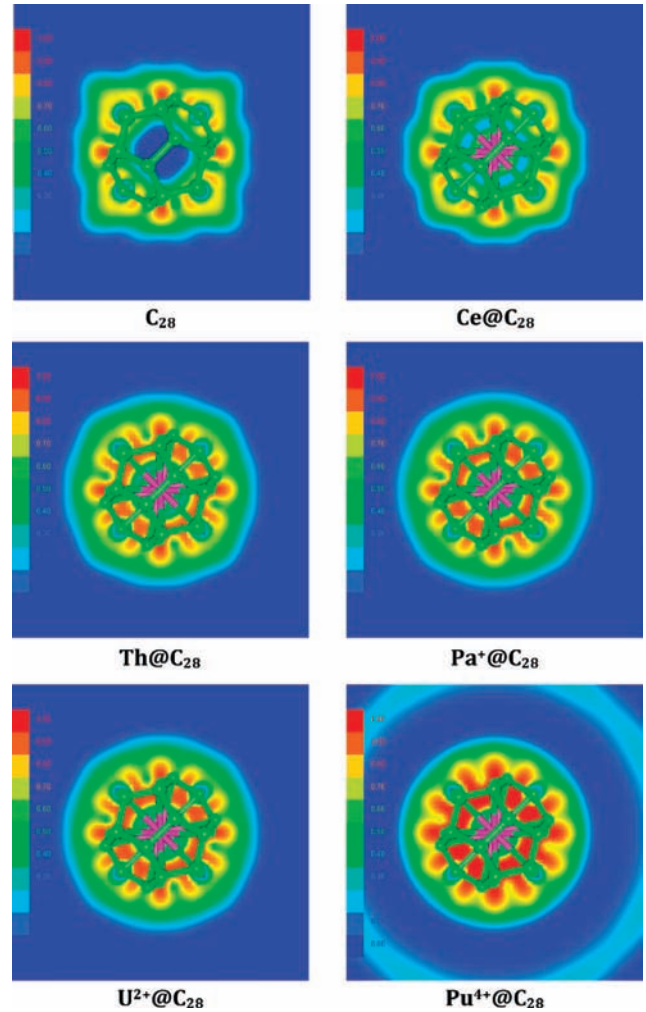

Figure 5. Cut-plane ELF representations for the C_{28} cage and the M@C_{28} clusters (M = Ce, Th, Pa^{+}, U^{2+}, Pu^{4+}). The red color corresponds to a local electron maximum.

(17) te Velde, G.; Bickelhaupt, F. M.; Baerends, E. J.; Fonseca Guerra, C.; van Gisbergen, S. J. A.; Snijders, J. G.; Ziegler, T. *J. Comput. Chem.* **2001**, *22*, 931–967.
(18) Fernando, G. W.; Sevilla, E. H.; Cooper, B. R. *Phys. Rev. B* **2000**, *61*, 12562–12565.

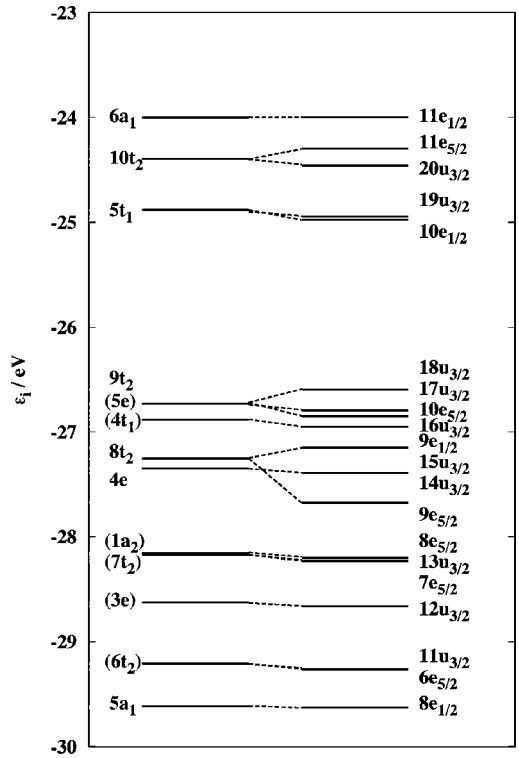

Figure 6. Occupied scalar relativistic valence orbital energy levels for the T_d Pu@C_{28} cluster (left) without and (right) with spin−orbit coupling. This is a 60-electron diagram that includes the 32-electron system ($6a_1$, $10t_2$, $5t_1$, $9t_2$, $8t_2$, 4e, $5a_1$) plus (in parentheses) the 28-electron "pure carbon" system (5e, $4t_1$, $1a_2$, $7t_2$, 3e, $6t_2$).

2.7 to 2.4 eV. There is no effect on the 5f orbital occupation compared to the PBE scalar relativistic values. For the bonding energy decomposition, decreases of less than 3% in both the steric and orbital interactions increases the absolute value of the total bonding energy by 2.9 eV. The global interpretation of the bonding energy analysis remains the same. Geometric and energetic properties are slightly affected by spin−orbit coupling effects. However, one can suppose that these effects may be larger on the MO splittings. Figure 6 shows the valence MO diagram for the Pu^{4+}@C_{28} cluster with T_d symmetry. The splittings are small in general, and the most significant splittings are obtained in the case of the $9t_2$ and $8t_2$ MOs, with values of 0.3 and 0.5 eV, respectively. They correspond to a mixing of 6d and 7p orbitals with the 2p(C) orbitals of the cage. We conclude that spin−orbit coupling effects are "diluted" by the presence of the fullerene cage and that there are no large effects on the ground-state molecular properties. Moreover, the spin−orbit coupling does not invalidate the previous conclusions about the 32-electron principle.

4. Spectroscopic Properties. Vibrational. Computed harmonic vibrational frequencies for the C_{28} cage and the M^{n+}@C_{28} clusters are given in Table 2. Because of the T_d symmetry, only T_2 frequencies are IR-active. The central atom in the fullerene has a strong influence on the spectrum. An intense peak is present with a maximum near 345 cm^{-1} for Pu^{4+}@C_{28}. Contrary to our prior results for An@ Pb_{12} or, for example, in CH_4@C_{84},[19] this peak does not arise from a simple particle-in-a box translation. The mode can be assigned to combined motions of the cage and of the central atom in the cage. Moreover, this

(19) Rehaman, A.; Gagliardi, L.; Pyykkö, P. *Int. J. Quantum Chem.* **2007**, *107*, 1162–1169.

Table 2. Calculated Harmonic Vibrational Frequencies (cm^{-1}) for the C_{28} Cage and the M@C_{28} Clusters (Absorption Intensities in km/mol Are Reported in Parentheses)

C_{28} cage	Ce@C_{28}	Th@C_{28}	Pa^{+}@C_{28}	U^{2+}@C_{28}	Pu^{4+}@C_{28}
392 (2)	324 (3)	306(0)	314 (3)	326 (8)	345 (45)
520 (0)	527 (1)	550 (1)	545 (0)	537 (0)	513 (0)
689 (5)	642 (1)	658 (2)	658 (1)	654 (0)	639 (0)
703 (1)	755 (4)	756 (0)	762 (1)	765 (1)	762 (0)
760 (1)	774 (20)	770 (25)	783 (6)	790 (0)	784 (9)
783 (8)	789 (0)	800 (1)	803 (0)	802 (0)	795 (9)
971 (12)	796 (0)	803 (2)	812 (3)	814 (4)	813 (2)
1078 (1)	936 (0)	911 (1)	945 (1)	968 (1)	979 (1)
1180 (15)	1060 (2)	1035 (1)	1069 (1)	1093 (1)	1103 (0)
1249 (18)	1107 (4)	1075 (7)	1113 (5)	1140 (3)	1153 (0)
1377 (17)	1238 (0)	1202 (3)	1244 (0)	1274 (0)	1289 (0)
	1280 (33)	1246 (32)	1287 (24)	1319 (12)	1343 (0)

mode is sensitive to the ion−cage bonding. In the Pu^{4+} cluster, the cage is smaller in size and close in size to the empty cage. Therefore, the Pu^{4+}−cage interaction is more pronounced, as seen from the high intensities for these central-atom-motion modes. From Th to Pu^{4+}, the displacement of the band related to this mode is in line with the increase of the bonding energy given in Figure 2. Experimentally, a characteristic intense band might be detected in the case of the plutonium 32-electron cluster. A medium band is also observed in the calculated uranium cluster IR spectrum. For empty C_{28}, the mode at 392 cm^{-1} corresponds to deformation of the cage.

All of the other vibrational frequencies for the cage and the clusters can be assigned to the motion of the cage (torsion and C−C modes).

Electronic. Time-dependent density functional theory (TD-DFT) as implemented in the ADF program package was used to compute electronic vertical singlet excitation energies with the PBE functional. Our goal was not to produce an extensive analysis of the electronic spectra but rather to find the character and the position of the main absorption bands and to provide an illustration of the optical properties for the Pu^{4+}@C_{28} cluster. In T_d point-group symmetry, only excitations having T_2 symmetry are allowed. The results without and with spin−orbit coupling are displayed in Figure 7 and compared with those for the C_{28} cage.

For the C_{28} cage, a strong absorption in the ultraviolet at ∼355 nm is calculated. Without spin−orbit coupling, as a result of the encapsulation of actinide, the absorption is slightly shifted toward the visible (380 nm). The introduction of spin−orbit coupling in the calculation gives absorptions in the blue (470−475 nm) and green (525 nm) regions of the visible spectrum with substantially decreased oscillator strength (Figure 7, right y axis). For the Pu^{4+}@C_{28} clusters, the major MOs involved in the excitations are 5f(Pu)/2p(C) hybrids without and with spin−orbit coupling. Thus, because of the large role of the spin−orbit coupling on the electronic spectra, further extended theoretical work including spin−orbit coupling will be necessary for a quantitative comparison with future experimental data.

5. Estimation of the Thermodynamic Stabilities of M@C_{28} Clusters. DFT harmonic vibrational frequencies and standard statistical thermodynamics (assuming ideal gas) can be used to estimate the enthalpies and entropies for the metal encapsulation reaction M^{n+} + C_{28} → M^{n+}@C_{28}. The results of ADF DFT/PBE calculations are collected in Table 3. The calculated reaction enthalpies ($\Delta_r H$) and Gibbs free energies ($\Delta_r G$) for M^{n+} encapsulation in a C_{28} cage are exothermic and account for a

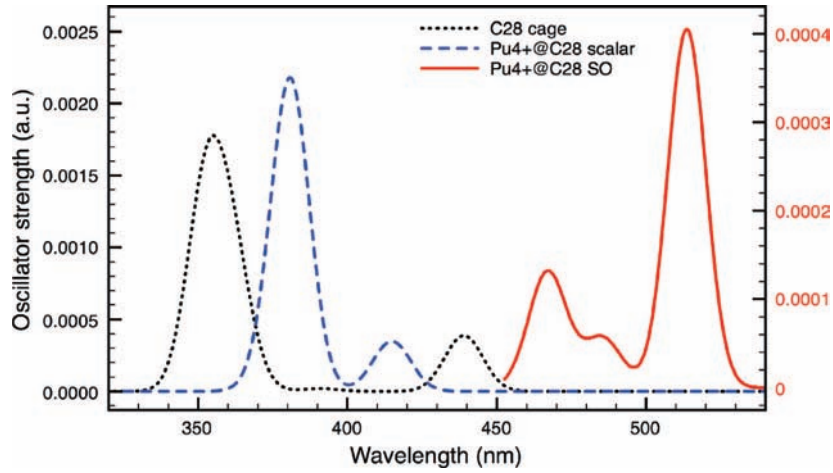

Figure 7. TD-DFT (PBE functional) UV−visible spectra for $Pu^{4+}@C_{28}$ (blue) without and (red, right *y* axis) with spin−orbit coupling compared with the C_{28} cage spectrum (black). The band shapes are approximated by Gaussian functions with a full width at half-maximum of 15 nm.

Table 3. DFT/PBE Reaction Enthalpies and Reaction Gibbs Free Energies (kJ/mol) for M^{n+} Encapsulation in C_{28} Cages ($T = 298.15$ K, $P = 1$ atm)

reaction	$\Delta_r H$	$\Delta_r G$
$Ce + C_{28} \rightarrow Ce@C_{28}$	−1181	−1123
$Th + C_{28} \rightarrow Th@C_{28}$	−1440	−1385
$Pa^{+} + C_{28} \rightarrow Pa^{+}@C_{28}$	−1431	−1373
$U^{2+} + C_{28} \rightarrow U^{2+}@C_{28}$	−3636	−3577
$Pu^{4+} + C_{28} \rightarrow Pu^{4+}@C_{28}$	−3641	−3582

great stability of the clusters ($T = 298.15$ K, $P = 1$ atm), particularly for the $U^{2+}@C_{28}$ and $Pu^{4+}@C_{28}$ cases. The reaction entropy ($\Delta_r S$) is nearly the same for all of the clusters, with a value of 190−200 J K^{-1} mol^{-1}. The origin of the stabilization of these clusters can be found in the orbital interaction between the actinide and the C_{28} cage and, especially in the case of U^{2+} and Pu^{4+}, in the large 5f contribution to the interaction.

Conclusions

In this study, we have proposed a new class of closed-shell organometallic species combining a central actinide atom inside the smallest known fullerene cage, C_{28}. The very stable character of these clusters was revealed by geometric and energetic criteria. Moreover, $Th@C_{28}$, $Pa^{+}@C_{28}$, $U^{2+}@C_{28}$, and $Pu^{4+}@C_{28}$ qualify as new examples of 32-electron species, in addition to our previous $An@Pb_{12}$ clusters. This raises an isolated curiosity to a principle. Moreover, the already experimentally known neutral cluster $U@C_{28}$ is shown to have a similar 32-electron bonding system. Specific spectroscopic fingerprints are provided. These clusters may have applications in novel cluster-based materials with continuously tunable electronic, magnetic, or optical properties across the 5f block.

Acknowledgment. P.P. belongs to the Finnish Center of Excellence (CoE) in Computational Molecular Science (2006−2011). The Center of Scientific Computing (CSC, Espoo, Finland) is acknowledged for providing computer resources. We thank the international program of the Ecole Polytechnique (Palaiseau, France) for supporting a one-month stay in France by P.P. This work was carried out in the framework of a collaboration between the French CEA-Direction des Sciences de la Matière and the University of Helsinki.

JA806811P